Materials and Structures (2022) 55:166
https://doi.org/10.1617/s11527-022-02002-x

ORIGINAL ARTICLE

Effect of temperature variations on the bond behavior of FRCM applied to masonry

Francesca Ferretti · Matteo Canestri · Claudio Mazzotti

Received: 25 April 2022 / Accepted: 26 June 2022 / Published online: 13 July 2022

Abstract In the last decades, Fiber Reinforced Cementitious Matrix (FRCM) composites were successfully introduced to repair and strengthen existing masonry structures. The good mechanical performances of these materials determined their efficiency as a strengthening technique; however, their durability is still an open issue. As a matter of fact, FRCM composites may be exposed to a combination of different environmental conditions and, additionally, to temperature variations due to solar radiation. The objective of this research was to study the effects of temperature variations on the bond behavior of a FRCM composite, constituted by a basalt grid and a lime-based mortar matrix, applied to masonry. For this purpose, an experimental investigation on thermally conditioned FRCM-strengthened masonry wallets is presented, in which 14 single-lap shear tests were performed. Before testing, samples were exposed to different target temperatures inside a climatic chamber: 32, 40, 50, 60 and 80 °C. Thermocouples were embedded within the FRCM reinforcing layers at two different depths to detect the inner temperature profiles and to control the conditioning process. The single-lap shear tests were then carried out inside the same climatic chamber, while maintaining the target temperature constant. A decrease in terms of peak-axial stress was observed by increasing temperature, along with a progressive change in the failure mode, from fiber rupture outside the bonded area to fiber slippage within the mortar matrix layers.

Keywords FRCM · Single-lap shear test · Bond behavior · Thermal variations · Thermal conditioning

F. Ferretti (✉) · M. Canestri · C. Mazzotti
Department of Civil, Chemical, Environmental and Materials Engineering, University of Bologna, Viale Risorgimento 2, 40136 Bologna, Italy
e-mail: francesca.ferretti10@unibo.it

M. Canestri
e-mail: matteo.canestri2@unibo.it

C. Mazzotti
e-mail: claudio.mazzotti@unibo.it

1 Introduction

Fiber Reinforced Cementitious Matrix (FRCM) composites were introduced as a retrofitting technique to repair and strengthen existing masonry constructions, usually highly vulnerable to seismic actions [1–7]. The use of these materials has progressively increased due to their effectiveness in improving both the in-plane and the out-of-plane behavior of masonry panels, as many research works demonstrated [8–16]. FRCM-strengthened masonry walls, indeed, are typically characterized by an increased load-bearing capacity and by a less fragile cracked behavior, with respect to unreinforced masonry elements [17–19]. At the structural system scale, the adoption of a variety of

materials was investigated [20] and, more recently, the use of natural fibers has gained attention [21–23].

Apart from the well investigated ultimate capacity of FRCM composites at failure [24–26], a further critical aspect to be considered when dealing with the design of strengthening interventions with FRCM systems is the durability of these materials. In fact, FRCM composites may be exposed to a combination of different aggressive environmental conditions, such as humidity, rainfall, freeze/thaw cycles, exposure to saline and alkaline environments, and to medium and high temperature. In this framework, several studies were recently conducted about the behavior of FRCM composites when subjected to aggressive environments, analyzing how these conditions could affect their mechanical performances [27–32]. At the same time, the *Italian Guidelines for the identification, qualification and acceptance control of FRCM composites to be used for the structural strengthening of existing constructions* [33] prescribe to evaluate the performances of these systems in presence of specific environmental actions.

Irrespective of the presence of an aggressive environment, lots of FRCM composites are bonded to the external surfaces of buildings, where the formers are directly exposed to the solar radiation and thus subjected to important temperature variations, whose effects on the efficiency of these composite materials might be relevant. Despite this common situation, limited studies have been conducted so far on the influence of sun-induced temperature variations on the mechanical behavior of FRCM systems [34, 35]. Few works focused on the analysis of the performances of FRCM composites by performing tensile and bond tests on samples subjected to very high temperatures, typically ranging from 100 to 500 °C, highlighting the influence of a strong thermal conditioning (close to the fire exposure) on the behavior of the different components, i.e., textile, mortar matrix, and matrix-to-textile interface [36–40]. The effect of lower temperatures, such as the ones that a FRCM composite could be subjected to under service conditions (e.g., intense sunlight exposure), has been less studied but should be further investigated, given the high probability of occurrence. In particular, recent research works [41, 42] focused on the tensile behavior of different FRCM composites exposed to temperature variations up to 80 °C and tested according to different experimental protocols: it was observed that an increase in temperature mainly impacted on the mortar matrix properties and on the matrix-to-textile interface behavior rather than on the textile performances. The organic content of both the mortar matrix and the coating applied to the fibers seemed to play an important role, especially in the matrix-to-textile interaction. For this reason, it is of great interest to investigate the influence of an increase in temperature on the bond behavior of these materials.

The objective of the present research was to analyze the effect of temperature variations on the bond behavior of a FRCM composite, composed by a basalt grid and a lime-based mortar matrix, applied to masonry. For this purpose, a series of single-lap shear tests were performed on 14 FRCM-strengthened masonry wallets. Besides the tests conducted at ambient temperature (23 °C) on 4 reference (unconditioned) specimens, single-lap shear tests were performed inside a climatic chamber at different target temperatures, namely 32, 40, 50, 60 and 80 °C. Inside the climatic chamber, prior to the test execution, two samples for each target temperature were subjected to a conditioning process, i.e., a heating phase followed by an exposure period in which the target temperature was maintained constant. Comparisons between the results of the different tests, in terms of bond behavior, strength and failure mode, will be thoroughly discussed in the following, showing an important role played by the temperature.

2 Description of the experimental campaign

2.1 Mechanical characterization of the materials

The FRCM composite investigated in the present experimental campaign was composed by a balanced basalt grid embedded inside a natural hydraulic lime-based mortar matrix. The basalt grid was characterized, in each direction, by a weight density of 210 g/m^2, by a yarn cross-section of 0.544 mm^2, by a grid spacing of 16 mm and by an equivalent thickness of 0.034 mm. Each single yarn of the grid was coated with an organic resin and the connection between longitudinal and transversal fibers was realized by heat-sealing (Fig. 1). The natural hydraulic lime-based mortar matrix was a pre-mixed mortar, characterized by the presence of organic compound, whose maximum content was equal to the 10% of the

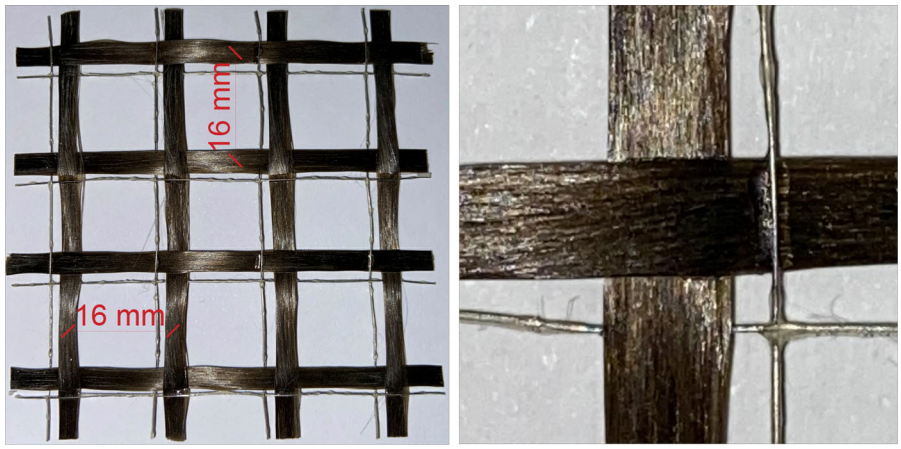

Fig. 1 Basalt bidirectional grid and detail of the heat-sealed connection between orthogonal fibers

inorganic binder, as declared by the producer. The FRCM composite was applied to 14 masonry wallets (see Sect. 2.2), realized by using 6 fired-clay bricks and a pre-mixed natural hydraulic lime-based mortar. The mechanical properties of all the materials were obtained through direct experimental testing, as described in the following.

2.1.1 Masonry

Fired-clay bricks, with dimensions 120 × 250 × 55 mm^3, were adopted to build the masonry wallets. Cylindrical samples, characterized by a diameter equal to 50 mm and by a unitary aspect ratio, were cored from the bricks: 12 cores were subjected to uniaxial compression test [43], and 12 cores were subjected to Brazilian test [44]. The brick compressive strength $f_{b,c}$ and the brick tensile strength $f_{b,t}$ resulted to be equal to 18.7 MPa (CoV 5.3%) and 3.1 MPa (CoV 15.3%), respectively. Cyclic compression tests [45] were also performed on 3 additional cylindrical specimens, having an aspect ratio of 2.5, to evaluate the brick elastic modulus E_b, equal to 6.9 GPa (CoV 3.9%).

To determine the mechanical properties of the mortar used for the construction of the masonry wallets, in terms of flexural strength, compressive strength and elastic modulus, three-points bending test, uniaxial and cyclic compression tests were carried out on prismatic specimens, according to European Standards [46]. In more detail, after 28 days of curing in the laboratory-controlled environment (T = 22 °C ± 1 °C, RH = 60% ± 5%), 10 mortar samples, with dimensions 160 × 40 × 40 mm^3, were subjected to three-points bending test, obtaining a mean flexural strength $f_{m,fl}$ = 1.5 MPa (CoV 15%); the 20 half prisms resulted from previous tests, where then subjected to uniaxial compression tests, obtaining a compressive strength $f_{m,c}$ = 4.8 MPa (CoV 12.5%). Cyclic compression tests were also performed on 3 prismatic specimens (dimensions of 160 × 40 × 40 mm^3) for the evaluation of the elastic modulus E_m, equal to 4.6 GPa (CoV 14.7%).

Results showed that the quality of the chosen masonry components, in terms of mechanical performances, can be considered representative of that of an existing masonry typology.

2.1.2 Mortar matrix

To evaluate the mechanical properties of the mortar matrix, the same procedures [45, 46] and type of specimens described in the previous section were used. The tests allowed to obtain the following mechanical properties: flexural strength $f_{mx,fl}$ = 8.1 MPa (CoV 2.3%), compressive strength $f_{mx,c}$ = 20.0 MPa (CoV 3.2%) and elastic modulus E_{mx} = 10.4 GPa (CoV 10.2%).

The effect of temperature variations on the mortar matrix properties was also investigated, by performing three-points bending tests on six additional specimens heated up to two different target temperatures, namely 50 and 80 °C. Before the test, carried out inside a climatic chamber (see Sect. 2.3), the temperature was increased at a rate of 30 °C/h until reaching the target threshold. A flexural strength $f_{mx,fl,T}$ equal to 6.4 MPa

(CoV 11.9%) and 4.0 MPa (CoV 8.6%), respectively for 50 and 80 °C, was obtained.

2.1.3 Textile

To perform the mechanical characterization of the textile, tensile tests were conducted on 9 bidirectional grid samples, following Italian and International Standard provisions [33, 47]. The samples, having dimensions 500 × 64 mm^2, were characterized by the presence of 4 yarns (Fig. 1). To properly transfer the load from the testing machine to the samples, Fiber Reinforced Polymer (FRP) tabs were applied at both extremities of the specimens by using epoxy resin. Tests were performed under displacement-control with a stroke rate of 0.5 mm/min (0.0083 mm/s) and by using a servo-hydraulic machine (100 kN capacity). An extensometer, having a gauge length of 200 mm, was used to register deformations of the central part of the grid samples. The average tensile strength $\sigma_{u,f}$, ultimate strain $\varepsilon_{u,f}$, and fiber elastic modulus E_f obtained from the tests were equal to 1201 MPa (CoV 3.1%), 1.97% (CoV 3.1%) and 78 GPa (CoV 3.5%), respectively.

2.1.4 Tensile tests on FRCM coupons

The tensile performances of the FRCM composite were also studied by means of direct tensile tests on 5 specimens, having dimensions 500 × 64 × 10 mm^3 and being characterized by the same number of yarns (4) considered in the tensile tests on the textile. After casting, samples were cured in the laboratory-controlled environment for 28 days before testing. The tests were performed under displacement control, using the same apparatus described in Sect. 2.1.3, at a stroke rate of 0.2 mm/min (0.0033 mm/s) until stabilization of the cracking process and of 0.5 mm/min (0.0083 mm/s) subsequently. An extensometer with a gauge length equal to 200 mm was applied in the center of the specimens to monitor the deformations during the tests. The extremities of the FRCM coupons were strengthened by FRP composite tabs to avoid local failures due to the hydraulic grips pressure. In Table 1, the axial stress and strain at first cracking (σ_{cr}, ε_{cr}) are reported, together with their values at failure (σ_u, ε_u). A typical trilinear behavior was observed for all the FRCM coupons [48–50]. Recognizing that the slope of the third branch of the σ–ε curve is mostly governed by the fiber elastic modulus, it was reported in Table 1 as E_f. The fiber rupture after the mortar matrix cracking was observed in all the tests. This failure mode is typical of tensile tests performed by using hydraulic gripping devices at the extremities of the samples, contrary to the adoption of clevis type grip systems, with which internal debonding/delamination is typically expected.

2.2 Preparation of the specimens for single-lap shear tests

The masonry wallets were built by stacking 6 bricks (250 × 120 × 55 mm^3), separated by 10-mm thick mortar joints, obtaining a total height of the specimens equal to 380 mm. The wallets were then cured in the laboratory-controlled environment for 28 days. After the curing process, the FRCM composite was applied to one of the wide faces (width 250 mm) of the masonry specimens, following the Recommendation of the RILEM Technical Committee 250-CSM [51]: the adopted bond length (l) was 300 mm, suggested as a good value for most of the available FRCM systems, while the reinforcement width (b_f) was 64 mm, so that to include four yarns; the thickness of the FRCM composite (t_f) was 10 mm and the bonded length started 30 mm far from the loaded edge of the wallet.

Before applying the FRCM composite, the masonry substrate surface was scraped with a metal wire brush and then it was cleaned with compressed air to remove the dust and improve the substrate-to-matrix adhesion. A first mortar matrix layer, 5-mm thick, was casted on the masonry surface, which was previously soaked (Fig. 2a) to prevent water depletion of the former. Then, the 64-mm wide basalt grid was gently pressed on top of the casted surface for a total length of 300 mm, while 430 mm of bare grid was left outside the bonded region (Fig. 2b). Finally, a second mortar matrix layer, 5-mm thick, was casted above the grid (Fig. 2c). All the FRCM-strengthened masonry wallets were then cured in the laboratory-controlled environment for 28 days before performing the single-lap shear tests.

With the intention of monitoring the temperature profile inside the FRCM composite, both in the conditioning and testing phases, five specimens were equipped with two K-type thermocouples, embedded inside the mortar matrix at two different depths: one was placed at the substrate-to-matrix interface

Table 1 Results of direct tensile tests on FRCM coupons

Sample ID	σ_{cr} (MPa)	ε_{cr} (%)	σ_u (MPa)	ε_u (%)	E_f (GPa)
TT_1	678	0.019	1257	1.312	84
TT_2	735	0.020	1196	1.191	81
TT_3	742	0.018	1289	1.353	71
TT_4	803	0.020	1302	1.130	74
TT_5	943	0.021	1350	1.153	76
Average	780	0.020	1279	1.224	77
CoV (%)	13.0	5.8	4.5	8.4	6.8

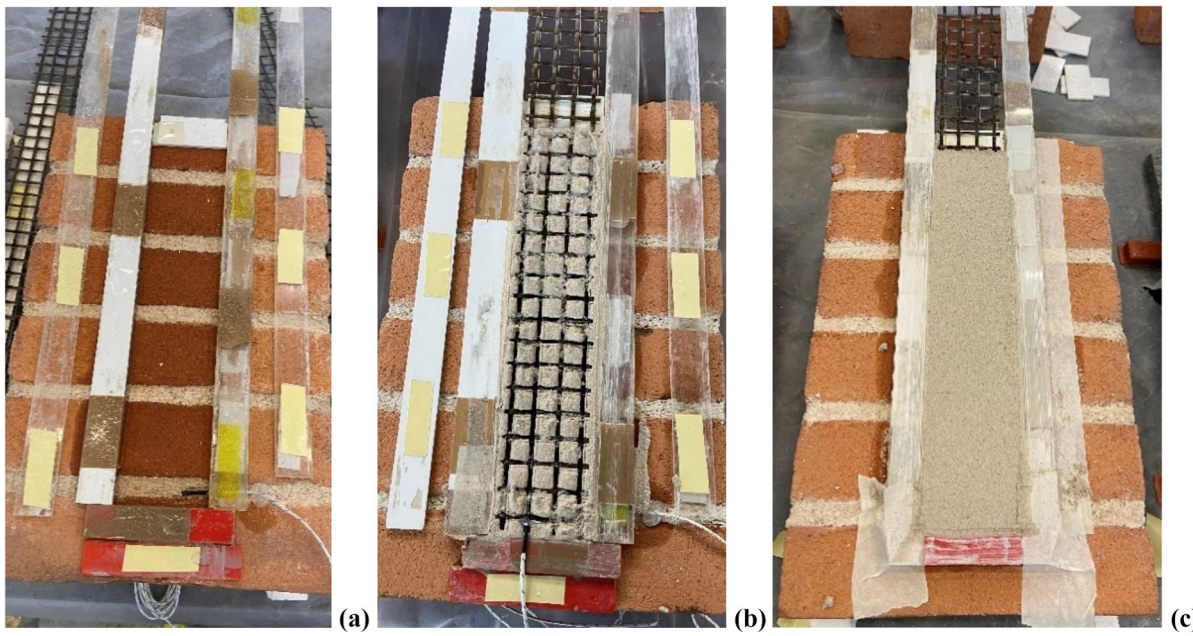

Fig. 2 Preparation of the specimens: **a** water-soaked substrate, **b** application of the first mortar matrix layer and basalt grid, **c** application of the second mortar matrix layer

(*TC_Interface* in the following), while the other was placed in direct contact with the basalt grid (*TC_Net* in the following). Since the cross-section dimensions of the cables of the thermocouples could potentially affect the load transfer mechanism, both instruments were positioned at the extremity of the FRCM reinforcing strip far from the loaded edge (Fig. 3), where the bond deformation are expected to be small or negligible [51–54].

2.3 Single-lap shear test setup and thermal conditioning procedure

To assess the bond behavior of the basalt FRCM composite applied on the masonry wallets, the single-lap shear test setup was adopted (Fig. 4a, b). Following a standard configuration, the textile was pulled by a servo-hydraulic actuator with a capacity of 100 kN, while the masonry wallet was restrained by a rigid steel frame, preventing the vertical displacements of the specimens. The masonry wallets were carefully positioned within the test setup to minimize potential force eccentricities. With the aim to promote a homogeneous stress distribution among all the yarns, the unbonded bare grid, 430-mm long, was impregnated with a bi-component epoxy resin and reinforced with FRP tabs in correspondence with the gripping area. All the tests were conducted under displacement control, at a rate of 0.15 mm/min (0.0025 mm/s). The applied load was measured with a class 0.5 load cell

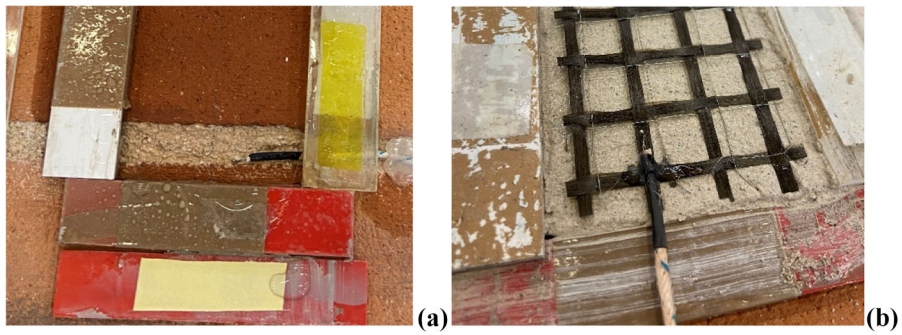

Fig. 3 Thermocouples embedded inside the FRCM reinforcement: **a** substrate-to-matrix interface (*TC_Interface*), **b** in contact with the basalt grid (*TC_Net*)

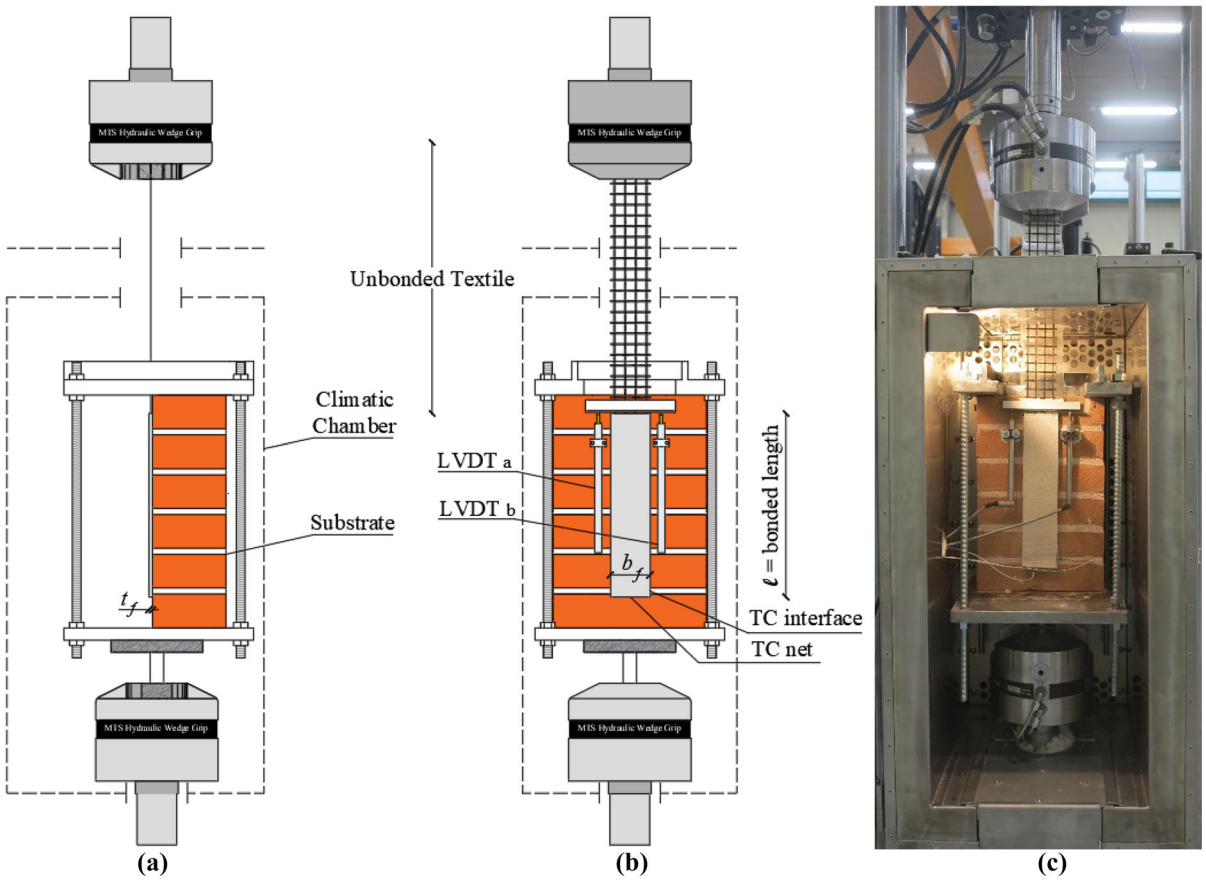

Fig. 4 Single-lap shear test setup: schematic **a** lateral and **b** front view, **c** specimen inside the climatic chamber

while the relative displacement between the textile and the masonry substrate, indicated as *global slip* in the following, was obtained by averaging the values registered by two 20-mm Linear Variable Displacement Transducers (LVDT). Both instruments were fixed to the masonry substrate and pointed against a thin L-shaped aluminum plate, glued to the part of the bare fibers immediately outside the bonded area.

A total of 14 single-lap direct shear tests were carried out: four of them, used as reference, were conducted at ambient temperature (23 °C), while the remaining samples were thermally conditioned and

tested at five different temperatures: 32, 40, 50, 60 and 80 ± 2 °C. All these values represent a possible in-situ condition of the FRCM composites and were chosen to investigate the effects of mild to intense solar radiation. Two test repetitions were performed for each target temperature. The specimens were identified with the notation "DS_*YY*_*X*", where the first two letters indicate the type of test (Direct Shear), *YY* the target temperature and *X* the specimen number.

Except for the reference specimens, the single-lap shear tests were executed inside a climatic chamber (Fig. 4c). This device allowed to recreate specific thermal conditions, within its operating temperature range of −129 °C and + 315 °C, with precise temperature management control and rapid heat transfer through forced convection heating. In this way, a controlled thermal gradient was prescribed to heat the conditioned specimens up to specific target temperatures, minimizing differences between the four exposed lateral surfaces of the masonry wallets. Mineral wool was used to fill the hole in the roof of the climatic chamber to ensure a proper control of the heating environment. The heating process was characterized by a first phase in which the temperature inside the climatic chamber was increased up to the target threshold with a heating rate equal to 30 °C/h, according to the indications provided by the Italian Guidelines [33] for tensile tests. Then, the temperature was maintained constant for a certain time frame, denoted in the following as *exposure period*, before the execution of the single-lap shear tests. Given that a standard test protocol is not available for bond tests under imposed temperature, it was decided to consider a variable duration of the exposure period for tests conducted at different temperatures. Specifically, it was extended until both the thermocouples reached a temperature equal to 95% of the target temperature. Once the exposure period was identified for one sample per target temperature, the test repetition at the same temperature was performed by imposing the same conditioning procedure.

3 Experimental results and discussion

3.1 Temperature profiles

During the heating process, the temperature inside the FRCM composite was registered by means of two embedded thermocouples (*TC_Net* and *TC_Interface*). In addition, the temperature of the air inside the climatic chamber was measured through a built-in sensor. With these data, temperature profiles were measured and reported in Fig. 5 as a function of time. Continuous and dotted lines for each target temperature represent data from the thermocouples, while the dash-dotted lines represent the imposed temperature inside the climatic chamber. In all cases, the heating process of the FRCM composite was quite fast at the beginning of the heating phase and it progressively slowed down approaching the target temperature: the amount of time required to reach a roughly constant temperature was different among the specimens, because it depended on the difference between the initial and the target temperature. The exposure time and the total duration of the heating and the testing phase are reported in Table 2 for each target temperature.

3.2 Single-lap shear test results

The results of the single-lap shear tests are reported in Table 3 in terms of peak-load, peak-axial stress, and failure mode. Peak-axial stress values were obtained by dividing the peak-load by the cross-section of the dry textile along the longitudinal direction (equal to 2.176 mm^2). Conditioned specimens showed significant strength reductions when the target temperature was increased; in particular, an average strength decrease, with respect to the unconditioned values, of 67, 58, 35, 30 and 18% was measured for samples tested at 80, 60, 50, 40 and 32 °C, respectively. This clear trend is also displayed in the graph reported in Fig. 6, where the peak-axial stresses were plotted against the target temperatures.

In Table 3, failure modes are listed according to the classification proposed in previous literature works [55, 56] and reported in Fig. 7, and a schematic indication of the behavior at failure of each single yarn is shown in Fig. 8. The position of the *TC_Net* thermocouple is also indicated. When increasing the target temperature, a progressive shift in the failure mode was clearly detected, with a growing number of yarns progressively slipping within the mortar matrix instead of breaking outside the bonded area. This is the effect of the increased temperature, which most probably softened the internal bond between the fibers and the surrounding mortar, as also observed in a

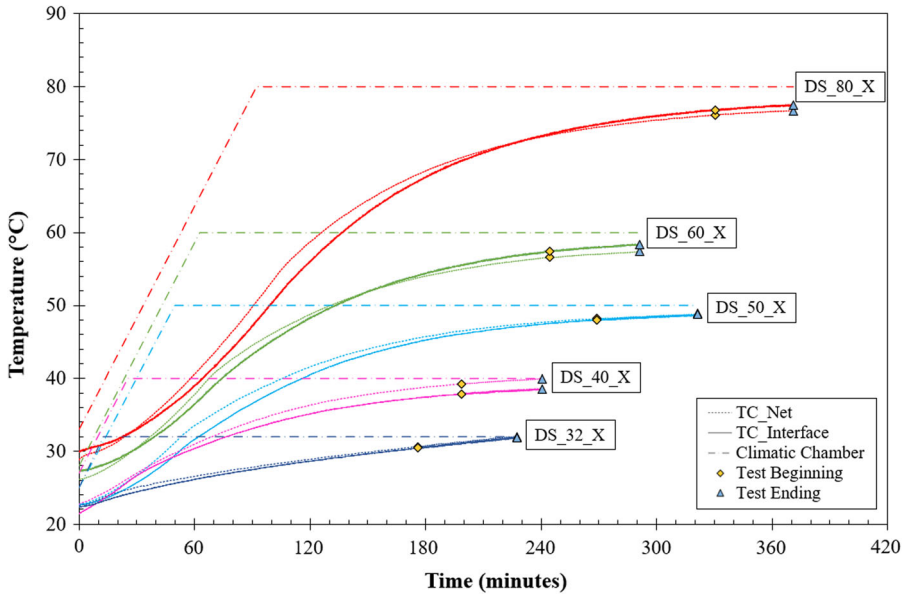

Fig. 5 Temperature variation with time at the different target temperatures within the FRCM composites (*TC_Net* and *TC_Interface*) and inside the climatic chamber

Table 2 Thermal conditioning procedures

Code	Number of samples	Target temperature (°C)	Exposure time (min)	Total duration (min)
DS_REF_X	4	23	–	–
DS_32_X	2	32	165	230
DS_40_X	2	40	175	240
DS_50_X	2	50	220	320
DS_60_X	2	60	180	290
DS_80_X	2	80	240	370

previous experimental campaign about the tensile behavior of FRCM composites subjected to temperature variations [42].

Figure 9 shows representative failure modes, observed for one reference and two conditioned samples. To better appreciate the different mechanisms, the external mortar matrix layer was gently removed from the rear part of the FRCM composite strip, exposing the last portion of the textile. For the reference samples, tensile failure occurred in the textile just outside the bonded area (Fig. 9a), with stress values similar to the strength of the textile (see Sect. 2.1.3). Specimens tested with target temperatures of 60 and 80 °C showed a completely different behavior, with predominant fiber slippage within the mortar matrix (Fig. 9b). Since the exposed portions of the yarns is at the rear extremity of the bonded area, a slippage located in this zone indicates that the whole yarn slipped while keeping its continuity along the "theoretical" bonded part. Finally, samples subjected to intermediate temperature levels, ranging from 32 up to 50 °C, exhibited a mixed failure mode, characterized by the rupture of some yarns and by the slippage of the remaining ones (Fig. 9c); even the yarns which ruptured, did that at a certain distance from the loaded edge (see upper yarn of Fig. 9c). It is worth mentioning that, in all cases, transversal yarns remained bonded to the mortar matrix, while longitudinal yarns moved consistently with the different failure modes. No visible cracks appeared on the external surface of the mortar matrix, in all the tested specimens.

Table 3 Single-lap shear test results

Sample ID	Target temperature (°C)	Peak load (kN)		Peak axial stress (MPa)		Failure mode
DS_REF_1	23	2.54	2.51*	1168	1157*	FR
DS_REF_2	23	2.57		1179		FR
DS_REF_3	23	2.49		1143		FR
DS_REF_4	23	2.48		1139		FR
DS_32_1	32	2.07	2.06*	953	944*	FS-FR**
DS_32_2	32	2.04		936		FS-FR**
DS_40_1	40	1.85	1.76*	849	811*	FS-FR**
DS_40_2	40	1.68		772		FS-FR**
DS_50_1	50	1.49	1.64*	685	754*	FS-FR**
DS_50_2	50	1.79		824		FS-FR**
DS_60_1	60	1.01	1.06*	464	488*	FS-FR**
DS_60_2	60	1.12		512		FS
DS_80_1	80	0.81	0.83*	369	381*	FS
DS_80_2	80	0.85		392		FS

*Average values, **Mixed failure mode

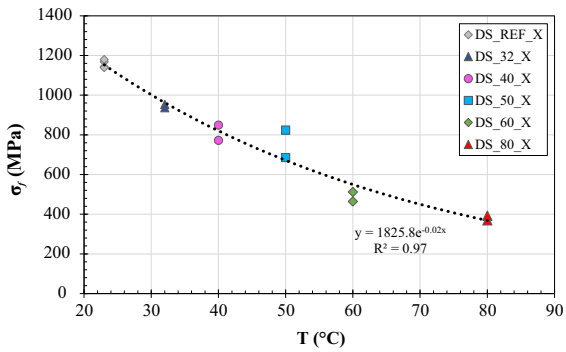

Fig. 6 Peak axial stress *vs* temperature

Figure 10 shows the obtained results in terms of axial stress *vs* global slip curves. In all cases, the first branch up to the peak was non-linear, with a non-linearity growing with the imposed temperature. Specimens tested at ambient temperature were characterized by a brittle behavior, with the tensile failure of the yarns just outside the bonded area. For the thermally conditioned specimens, instead, in the post-peak phase a softening behavior was observed, produced by the growing number of yarns which slipped inside the mortar matrix. The brittleness of these curves is roughly related to the intensity of the target temperature: the higher the temperature the lower the brittleness; this behavior was typical for specimens conditioned and tested at 60 and 80 °C. The sudden vertical stress drops, visible especially for samples conditioned and tested at low target temperatures, were produced by the tensile rupture of single yarns outside the bonded area. Samples tested with the same target temperature showed a similar global slip at peak. Only the couple of specimens DS_32_X and DS_50_X showed different values of global slip at peak between the two tested samples. In fact, the mixed failure mode characterizing the specimens tested at intermediate temperatures might lead to a different behavior at peak (e.g., if fibers slippage occurred—or not—before the tensile failure of one of the yarns), increasing the corresponding range of slip at peak, given a target temperature. For this reason, the reliability of this parameter as a comparison index was questionable and consequently not considered in the discussion of the results.

Based on the presented results, it can be noticed that, for the unconditioned specimens, the bond between the textile and the mortar matrix was good and the exploitation of the tensile capacity of the former was fully achieved, providing high values of peak-axial stress before the rupture of the fibers. By increasing the target temperature, the bond behavior of the yarns changed significantly, both in terms of bond strength and failure mode. This could be explained by

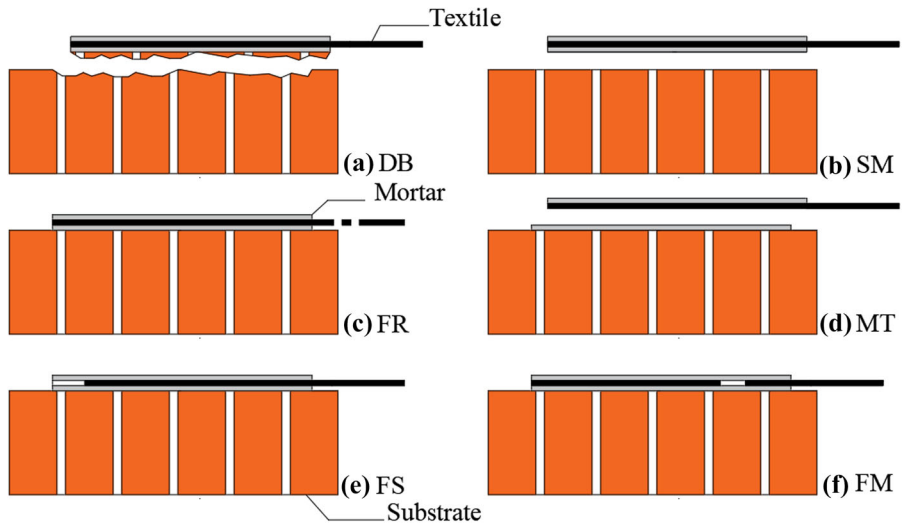

Fig. 7 Failure modes for FRCM composites subjected to single-lap shear test: **a** debonding of the reinforcement strip with failure of the substrate (DB), **b** debonding at the substrate-to-matrix interface (SM), **c** fibers rupture outside the bonded area (FR), **d** delamination at the matrix-to-textile interface (MT), **e** fibers slippage within the mortar matrix layers (FS), **f** fibers rupture inside the bonded area (FM)

Yarn	1	2	3	4
DS_REF_1	FR	FR	FR	FR
DS_REF_2	FR	FR	FR	FR
DS_REF_3	FR	FR	FR	FR
DS_REF_4	FR	FR	FR	FR
DS_32_1	FR	FS*	FS	FR
DS_32_2	FR	FR	FS	FR
DS_40_1	FR	FS*	FR	FS
DS_40_2	FR	FS	FS	FS
DS_50_1	FS	FR*	FS	FS
DS_50_2	FS	FR	FR	FS
DS_60_1	FR	FS*	FS	FS
DS_60_2	FS	FS	FS	FS
DS_80_1	FS	FS*	FS	FS
DS_80_2	FS	FS	FS	FS

FR Rupture
FS Slippage
* Thermocouple

Fig. 8 Failure mode of the single yarns in all tested specimens

considering that a temperature increase produces different simultaneous effects on the FRCM composite constituents. The most important one is determined on the organic components present both in the mortar matrix and in the fiber coating. These materials are generally thermoplastic materials, characterized by a low glass transition temperature, beyond which they become softer. For the mortar matrix, it was already observed that its flexural strength decreased by increasing temperature above 50 °C. The weakening of these materials, besides affecting their mechanical properties, detrimentally affected the matrix-to-textile interface bond as well. In addition, the temperature increase could have triggered an early rupture of the connections between longitudinal and transversal yarns, realized following a heat-sealing process, thus facilitating the fiber slippage.

4 Conclusions

In the present research, single-lap shear tests were performed on masonry wallets strengthened by means of a FRCM composite. Tests were performed inside a climatic chamber at different target temperatures, with the objective of studying the effect of an increase in temperature on the bond behavior of the FRCM composite, made by a basalt grid embedded within a natural hydraulic lime-based mortar matrix. The chosen target temperatures, between 30 and 80 °C, were compatible with the ones which could be produced by an intense solar radiation on the external surfaces of buildings.

Even though the experimental campaign was limited in terms of number and types of FRCM strengthening systems considered, the obtained results allowed to draw the following preliminary conclusions:

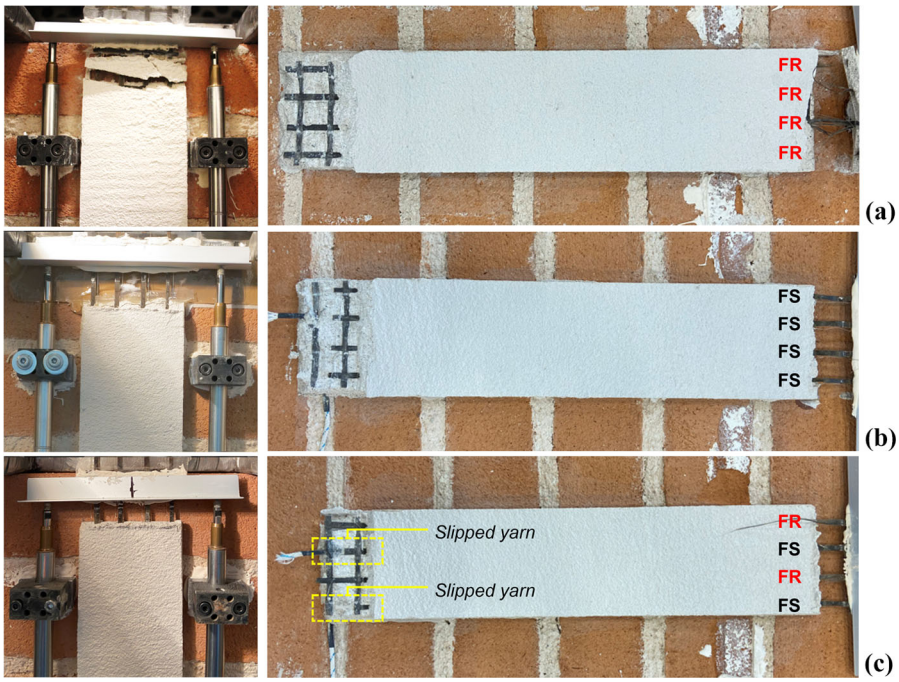

Fig. 9 Representative failure modes: **a** Fiber Rupture (DS_REF_01), **b** Fiber Slippage (DS_80_1), **c** mixed failure (DS_40_1)

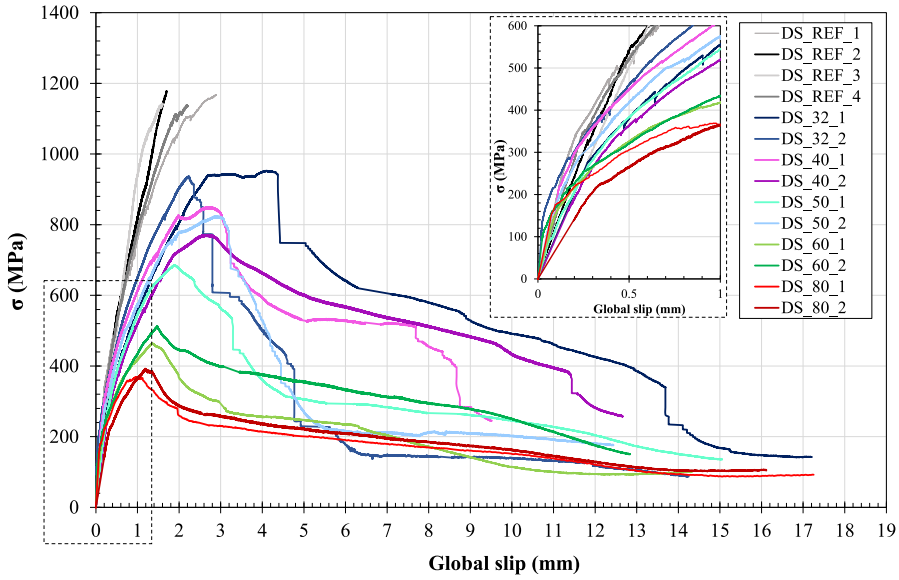

Fig. 10 Axial stress *vs* global slip curves

– A progressive decrease in terms of peak-axial stress was observed by increasing the target temperature, with significant strength reduction with respect to the unconditioned samples, up to 67% for specimens tested at 80 °C.
– The failure mode of the FRCM composite changed for conditioned specimens, shifting from complete fiber rupture outside the bonded area for unconditioned samples to complete fiber slippage within the mortar matrix for specimens heated up to 60 and 80 °C. A mixed failure mode, with both fiber rupture and slippage, was observed for the intermediate target temperatures.

– The effects produced by a temperature increase on both the organic coating applied to the fibers and the organic compound inside the mortar matrix, characterized by low glass transition temperatures, negatively affected the bond behavior at the matrix-to-textile interface, leading to a remarkable reduction of the composite performances.

Given that a standard testing procedure has not been defined yet for investigating the bond behavior of FRCM composites at specific temperatures, the testing procedure adopted in this experimental campaign can provide a basis for future research and standardization, i.e., the definition of appropriate exposure periods, which can be differentiated according to the target temperature which has to be prescribed to the FRCM composites. Finally, it should be also highlighted the importance of conducting the tests inside a climatic chamber to ensure a proper conditioning environment. The use of a climatic chamber could be crucial also for the analysis of the effects of freeze, for which low temperatures should be prescribed to the FRCM composites. These tests, whose outcomes might be interesting to achieve a comprehensive understanding of the behavior of these materials under service conditions, will be the object of future experimental studies.

Acknowledgements The financial support of the Italian Department of Civil Protection (ReLUIS 2022 Grant - Innovative Materials) is gratefully acknowledged. The technical staff at CIRI Buildings & Construction is gratefully acknowledged for the collaboration during the preparation and execution of the tests.

Funding Open access funding provided by Alma Mater Studiorum - Università di Bologna within the CRUI-CARE Agreement.

Declarations

Conflict of interest The authors declare that they have no conflict of interest.

References

1. Ceci AM, Contento A, Fanale L, Galeota D, Gattulli V, Lepidi M, Potenza P (2010) Structural performance of the historic and modern buildings of the University of L'Aquila during the seismic events of April 2009). Eng Struct 32:1899–1924. https://doi.org/10.1016/j.engstruct.2009.12.023
2. D'Ayala DF, Paganoni S (2011) Assessment and analysis of damage in L'Aquila historic city centre after 6th April 2009. Bull Earthq Eng 9:81–104. https://doi.org/10.1007/s10518-010-9224-4
3. Penna A, Morandi P, Rota M, Manzini CF, da Porto F, Magenes G (2014) Performance of masonry buildings during the Emilia 2012 earthquake. Bull Earthq Eng 12:2255–2273. https://doi.org/10.1007/s10518-013-9496-6
4. Ferretti, F, Mazzotti C, Esposito R, Rots JG (2018) Shear-sliding behavior of masonry: numerical micro-modeling of triplet tests. In: Comput. Model. Concr. Struct. CRC Press, Boca Raton, pp. 941–951. https://doi.org/10.1201/9781315182964-109.
5. Ferretti F, Ferracuti B, Mazzotti C, Savoia M (2019) Destructive and minor destructive tests on masonry buildings: experimental results and comparison between shear failure criteria. Constr Build Mater 199:12–29. https://doi.org/10.1016/j.conbuildmat.2018.11.246
6. Sorrentino L, Cattari S, da Porto F, Magenes G, Penna A, Seismic behaviour of ordinary masonry buildings during the 2016 central Italy earthquakes. Bull Earthq Eng 17:5583–5607. https://doi.org/10.1007/s10518-018-0370-4
7. C. Del Gaudio, S.A. Scala, P. Ricci, G.M. Verderame, Evolution of the seismic vulnerability of masonry buildings based on the damage data from L'Aquila 2009 event. Bull Earthq Eng 19:4435–4470. https://doi.org/10.1007/s10518-021-01132-x
8. Faella C, Martinelli E, Nigro E, Paciello S (2010) Shear capacity of masonry walls externally strengthened by a cement-based composite material: An experimental campaign. Constr Build Mater 24:84–93. https://doi.org/10.1016/j.conbuildmat.2009.08.019
9. Parisi F, Iovinella I, Balsamo A, Augenti N, Prota A (2013) In-plane behaviour of tuff masonry strengthened with inorganic matrix–grid composites. Compos Part B Eng 45:1657–1666. https://doi.org/10.1016/j.compositesb.2012.09.068
10. Babaeidarabad S, De Caso F, Nanni A (2014) URM walls strengthened with fabric-reinforced cementitious matrix composite subjected to diagonal compression. J Compos Constr 18:04013045. https://doi.org/10.1061/(ASCE)CC.1943-5614.0000441
11. Mininno G, Ghiassi B, Oliveira DV (2017) Modelling of the in-plane and out-of-plane performance of TRM-strengthened Masonry walls. Key Eng Mater 747:60–68. https://doi.org/10.4028/www.scientific.net/KEM.747.60

12. Bellini A, Incerti A, Bovo M, Mazzotti C (2018) Effectiveness of FRCM reinforcement applied to masonry walls subject to axial force and out-of-plane loads evaluated by experimental and numerical studies. Int J Archit Herit 12:376–394. https://doi.org/10.1080/15583058.2017.1323246
13. D'Ambra C, Lignola GP, Prota A, Fabbrocino F, Sacco E (2019) FRCM strengthening of clay brick walls for out of plane loads. Compos Part B Eng 174:107050. https://doi.org/10.1016/j.compositesb.2019.107050
14. Castori G, Corradi M, Sperazini E (2021) Full size testing and detailed micro-modeling of the in-plane behavior of FRCM–reinforced masonry. Constr Build Mater 299:124276. https://doi.org/10.1016/j.conbuildmat.2021.124276
15. Donnini J, Maracchini G, Lenci S, Corinaldesi V, Quagliarini E (2021) TRM reinforced tuff and fired clay brick masonry: Experimental and analytical investigation on their in-plane and out-of-plane behavior. Constr Build Mater 272:121643. https://doi.org/10.1016/j.conbuildmat.2020.121643
16. Garcia-Ramonda L, Pelà L, Roca P, Camata G (2022) Cyclic shear-compression testing of brick masonry walls repaired and retrofitted with basalt textile reinforced mortar. Compos Struct 283:115068. https://doi.org/10.1016/j.compstruct.2021.115068
17. Incerti A, Ferretti F, Mazzotti C (2019) FRCM strengthening systems efficiency on the shear behavior of pre-damaged masonry panels: an experimental study. J Build Pathol Rehabil 4:14. https://doi.org/10.1007/s41024-019-0053-9
18. Ferretti F, Incerti A, Tilocca AR, Mazzotti C (2021) In-plane shear behavior of stone masonry panels strengthened through grout injection and fiber reinforced cementitious matrices. Int J Archit Herit 15:1375–1394. https://doi.org/10.1080/15583058.2019.1675803
19. Ferretti F, Mazzotti C (2021) FRCM/SRG strengthened masonry in diagonal compression: experimental results and analytical approach proposal. Constr Build Mater 283:122766. https://doi.org/10.1016/j.conbuildmat.2021.122766
20. Del Zoppo M, Di Ludovico M, Prota A (2019) Analysis of FRCM and CRM parameters for the in-plane shear strengthening of different URM types. Compos Part B Eng 171:20–33. https://doi.org/10.1016/j.compositesb.2019.04.020
21. Olivito RS, Cevallos OA, Carrozzini A (2014) Development of durable cementitious composites using sisal and flax fabrics for reinforcement of masonry structures. Mater Des 57:258–268. https://doi.org/10.1016/j.matdes.2013.11.023
22. de Carvalho Bello CB, Boem I, Cecchi A, Gattesco N, Oliveira (2019) Experimental tests for the characterization of sisal fiber reinforced cementitious matrix for strengthening masonry structures. Constr Build Mater 219:44–55. https://doi.org/10.1016/j.conbuildmat.2019.05.168.
23. Cassese P, Balestrieri C, Fenu L, Asprone D, Parisi F (2021) In-plane shear behaviour of adobe masonry wallets strengthened with textile reinforced mortar. Constr Build Mater 306:124832. https://doi.org/10.1016/j.conbuildmat.2021.124832
24. Del Zoppo M, Di Ludovico M, Balsamo A, Prota A (2019) Experimental in-plane shear capacity of clay brick masonry panels strengthened with FRCM and FRM composites. J Compos Constr 23:04019038. https://doi.org/10.1061/(ASCE)CC.1943-5614.0000965
25. Murgo FS, Ferretti F, Mazzotti C (2021) A discrete-cracking numerical model for the in-plane behavior of FRCM strengthened masonry panels. Bull Earthq Eng 19:4471–4502. https://doi.org/10.1007/s10518-021-01129-6
26. Dalalbashi A, Ghiassi B, Oliveira DV (2021) A multi-level investigation on the mechanical response of TRM-strengthened masonry. Mater Struct 54:224. https://doi.org/10.1617/s11527-021-01817-4
27. Nobili A, Signorini C (2017) On the effect of curing time and environmental exposure on impregnated Carbon Fabric Reinforced Cementitious Matrix (CFRCM) composite with design considerations. Compos Part B Eng 112:300–313. https://doi.org/10.1016/j.compositesb.2016.12.022
28. Donnini J (2019) Durability of glass FRCM systems: effects of different environments on mechanical properties. Compos Part B Eng 174:107047. https://doi.org/10.1016/j.compositesb.2019.107047
29. Micelli F, Aiello MA (2019) Residual tensile strength of dry and impregnated reinforcement fibres after exposure to alkaline environments. Compos Part B Eng 159:490–501. https://doi.org/10.1016/j.compositesb.2017.03.005
30. Dalalbashi A, Ghiassi B, Oliveira DV (2021) Aging of lime-based TRM composites under natural environmental conditions. Constr Build Mater 270:121853. https://doi.org/10.1016/j.conbuildmat.2020.121853
31. Bellini A, Tilocca AR, Frana I, Savoia M, Mazzotti C (2020) Environmental durability of FRCM strengthening systems and comparison with dry fabrics. In: Proceedings of 17th international brick and block masonry conference, Krakow, Poland.
32. Dalalbashi A, Ghiassi B, Oliveira DV (2021) Influence of freeze–thaw cycles on the pull-out response of lime-based TRM composites. Constr Build Mater 313:125473. https://doi.org/10.1016/j.conbuildmat.2021.125473
33. Consiglio Superiore Lavori Pubblici, Linea Guida per la identificazione, la qualificazione ed il controllo di accettazione di compositi fibrorinforzati a matrice inorganica (FRCM) da utilizzarsi per il consolidamento strutturale di costruzioni esistenti (in Italian), CSLP (Consiglio Superiore dei Lavori Pubblici), Rome, Italy, 2018.
34. Ombres L (2015) Analysis of the bond between Fabric Reinforced Cementitious Mortar (FRCM) strengthening systems and concrete. Compos Part B Eng 69:418–426. https://doi.org/10.1016/j.compositesb.2014.10.027
35. Donnini J, De Caso y Basalo F, Corinaldesi V, Lancioni G, Nanni A (2017) Fabric-reinforced cementitious matrix behavior at high-temperature: experimental and numerical results. Compos Part B Eng 108:108–121. https://doi.org/10.1016/j.compositesb.2016.10.004.
36. Maroudas SR, Papanicolaou CCG (2017) Effect of high temperatures on the TRM-to-Masonry bond. Key Eng Mater 747:533–541. https://doi.org/10.4028/www.scientific.net/KEM.747.533
37. Ombres L, Iorfida A, Mazzuca S, Verre S (2018) Bond analysis of thermally conditioned FRCM-masonry joints. Measurement 125:509–515. https://doi.org/10.1016/j.measurement.2018.05.021
38. Iorfida A, Candamano S, Crea F, Ombres L, Verre S, de Fazio P (2019) Bond behaviour of FRCM composites:

effects of high temperature. Key Eng Mater 817:161–166. https://doi.org/10.4028/www.scientific.net/KEM.817.161
39. Askouni PD, Corina C, Papanicolaou G, Kaffetzakis MI (2019) The effect of elevated temperatures on the TRM-to-masonry bond: comparison of normal weight and light-weight matrices. Appl Sci 9:2156. https://doi.org/10.3390/app9102156.
40. Estevan L, Varona FB, Baeza FJ, Torres B, Bru D (2022) Textile Reinforced Mortars (TRM) tensile behavior after high temperature exposure. Constr Build Mater 328:127116. https://doi.org/10.1016/j.conbuildmat.2022.127116
41. Ferretti F, Tilocca AR, Incerti A, Mazzotti C, Savoia M (2022) Tensile behavior of FRCM coupons under thermal stresses. Key Eng Mater 916:50–57. https://doi.org/10.4028/p-rki9n6
42. Ferretti F, Tilocca AR, Incerti A, Mazzotti C, Savoia M (2022) (Forthcoming) Effects of thermal variations on the tensile behavior of FRCM strengthening systems. J Compos Constr. https://doi.org/10.1061/(ASCE)CC.1943-5614.0001241 (forthcoming)
43. EN 772-1, Methods of test for masonry units - Part 1: Determination of compressive strength, (2011).
44. EN 12390-6:2009, Testing hardened concrete - Part 6: Tensile splitting strength of test specimen, (2010).
45. EN 12390-13, Testing hardened concrete - Determination of secant modulus of elasticity in compression, (2013).
46. EN 1015-11, Methods of test for mortar for masonry—Part 11: Determination of flexural and compressive strength of hardened mortar, European Committee for Standardization, 2019.
47. ACI 549.6R-20, Design and construction of externally bonded Fabric-Reinforced Cementitious Matrix (FRCM) systems for repair and strengthening concrete and masonry Structures, American Concrete Instutute (ACI), 2020.
48. Leone M, Aiello MA, Balsamo A, Carozzi FG, Ceroni F, Corradi M, Gams M, Garbin E, Gattesco N, Krajewski P, Mazzotti C, Oliveira D, Papanicolaou C, Ranocchiai G, Roscini F, Saenger D (2017) Glass fabric reinforced cementitious matrix: tensile properties and bond performance on masonry substrate. Compos Part B Eng 127:196–214. https://doi.org/10.1016/j.compositesb.2017.06.028
49. Carozzi FG, Bellini A, D'Antino T, de Felice G, Focacci F, Hojdys Ł, Laghi L, Lanoye E, Micelli F, Panizza M, Poggi C (2017) Experimental investigation of tensile and bond properties of Carbon-FRCM composites for strengthening masonry elements. Compos Part B Eng 128:100–119. https://doi.org/10.1016/j.compositesb.2017.06.018
50. Lignola GP, Caggegi C, Ceroni F, De Santis S, Krajewski P, Lourenço PB, Morganti M, (Corina) Papanicolaou C, Pellegrino C, Prota A, Zuccarino L (2017) Performance assessment of basalt FRCM for retrofit applications on masonry. Compos Part B Eng 128:1–18. https://doi.org/10.1016/j.compositesb.2017.05.003.
51. de Felice G, Aiello MA, Caggegi C, Ceroni F, De Santis S, Garbin E, Gattesco N, Hojdys Ł, Krajewski P, Kwiecień A, Leone M, Lignola GP, Mazzotti C, Oliveira D, Papanicolaou C, Poggi C, Triantafillou T, Valluzzi MR, Viskovic A (2018) Recommendation of RILEM Technical Committee 250-CSM: Test method for Textile Reinforced Mortar to substrate bond characterization. Mater Struct 51:95. https://doi.org/10.1617/s11527-018-1216-x
52. D'Antino T, Carloni C, Sneed LH, Pellegrino C (2014) Matrix–fiber bond behavior in PBO FRCM composites: a fracture mechanics approach. Eng Fract Mech 117:94–111. https://doi.org/10.1016/j.engfracmech.2014.01.011
53. Bilotta A, Ceroni F, Nigro E, Pecce M (2017) Experimental tests on FRCM strengthening systems for tuff masonry elements. Constr Build Mater 138:114–133. https://doi.org/10.1016/j.conbuildmat.2017.01.124
54. Bellini A, Aiello MA, Bencardino F, de Carvalho Bello CB, Castori G, Cecchi A, Ceroni F, Corradi M, D'Antino T, De Santis S, Fagone M, de Felice G, Leone M, Lignola GP, Napoli A, Nisticò M, Poggi C, Prota A, Ranocchiai G, Realfonzo R, Sacco E, Mazzotti C (2021) Influence of different set-up parameters on the bond behavior of FRCM composites. Constr Build Mater 308:124964. https://doi.org/10.1016/j.conbuildmat.2021.124964.
55. Ascione L, de Felice G, De Santis S (2015) A qualification method for externally bonded Fibre Reinforced Cementitious Matrix (FRCM) strengthening systems. Compos Part B Eng 78:497–506. https://doi.org/10.1016/j.compositesb.2015.03.079
56. Valluzzi MR, Oliveira DV, Caratelli A, Castori G, Corradi M, de Felice G, Garbin E, Garcia D, Garmendia L, Grande E, Iannirubertо U, Kwiecień A, Leone M, Lignola GP, Lourenço PB, Malena M, Micelli F, Panizza M, Papanicolaou CG, Prota A, Sacco E, Triantafillou TC, Viskovic A, Zając B, Zuccarino G (2012) Round Robin Test for composite-to-brick shear bond characterization. Mater Struct 45:1761–1791. https://doi.org/10.1617/s11527-012-9883-5